Available online at www.sciencedirect.com
ScienceDirect
Catalysis Today 120 (2007) 96–106
CATALYSIS TODAY
www.elsevier.com/locate/cattod

Optimal reactor dimensions for homogeneous combustion in small channels

N.S. Kaisare, D.G. Vlachos *

Department of Chemical Engineering, Center for Catalytic Science and Technology, University of Delaware, Newark, DE, United States

Available online 23 August 2006

Abstract

This paper addresses the question of choosing the appropriate reactor length, wall thickness, and reactor opening size for self-sustained homogeneous combustion in parallel plate channels. First, the flame characteristics and stability of homogeneous combustion in micro-scale (<1 mm) and meso-scale (>1 mm) channels are studied, and the roles of heat recirculation and heat loss on the mechanisms of flame extinction and blowout are investigated. Based on these insights, the effects of reactor dimensions on flame stability are studied. Increasing the reactor length results in shrinking of the region of self-sustained combustion due to increased heat losses through the reactor solid structure. An optimum gap width in the range of ~600–1200 μm (transition from micro- to meso-scales) provides the largest region of self-sustained combustion. Size effects are stronger for methane than for propane combustion.

Keywords: Microburners; Flame stability; Homogeneous combustion; Blowout; Extinction; Propane; Methane

1. Introduction

Combustion in micro- and meso-scale channels lies at the heart of various portable power generation devices that could replace current batteries to meet the increasing demand for more efficient, longer lasting and more environmentally friendly operation of electronic and telecommunication devices in both civilian and military applications [1]. Combustion converts the chemical energy of fuels into thermal energy, which can then be harnessed as electricity in an integrated device via various alternate routes. Examples include integrated microreactors for generation of hydrogen for fuel cells via reforming [2–4] or ammonia decomposition [5,6], micro-turbines [7,8], thermo-electric devices [9,10], thermo-photovoltaics [11], etc.

For these devices to be convenient, reliable and commercially viable, on-demand generation of electricity under different operating conditions is required. Consequently, understanding the characteristics and the stability limits of combustion in micro- and meso-scale devices is essential in designing robust and efficient systems. Since Davy's seminal work two centuries ago [12], it has been widely accepted that there exists a critical dimension, of the order of 1 mm, below which flame propagation cannot be achieved due to thermal and radical quenching [13,14]. However, recent work has shown that it is possible to sustain homogeneous flames in sub-millimeter channels (hereafter termed micro-combustion) in specially constructed ceramic microburners [15].

There have been several studies on stability of homogeneous and catalytic combustion in micro- and mainly in meso-scale devices. Maruta et al. [16] studied the stability of catalytic combustion of methane–air mixtures, focusing on the effect of equivalence ratio and flow velocity on thermal quenching. Ronney [17] used a simplified model to study flame stability in heat recirculating Swiss-roll type burners. A straight channel system was also studied; however, an *a priori* assumption regarding the location of the flame was needed to obtain an analytical solution. Ju and Choi [18] presented an analytical solution of simplified mass and energy balance equations for counter-flow heat recirculating burners. To obtain an analytical solution, they made a "thin wall approximation," which may not hold for micro-scale burners, where the wall thickness is of the order of the gap width. Raimondeau et al. [19] studied the effect of radical and thermal quenching on flame propagation in microchannels. Norton and Vlachos [20,21] investigated the stability and thermal quenching of homogeneous premixed methane and propane flames in microchannels using a two-dimensional (2D) elliptic computational fluid dynamics (CFD) model. Leach and Cadou [22] used a simple heat resistor network analogy to obtain extinction limits. Although their model was

* Corresponding author. Tel.: +1 302 831 2830; fax: +1 302 831 1048.
E-mail address: vlachos@udel.edu (D.G. Vlachos).

0920-5861/$ – see front matter © 2006 Elsevier B.V. All rights reserved.
doi:10.1016/j.cattod.2006.07.036

Nomenclature

a	surface area (m^2)
a_{cs}	cross-sectional area of the solid plate (m^2)
b_w	wall thickness (m)
$\bar{c}_p$	specific heat (J/kg K)
d	gap width (m)
D	diffusivity (m^2/s)
h	coefficient of heat transfer/loss (W/m^2 K)
H	enthalpy or heat of reaction (J/mol)
k	thermal conductivity (W/m K)
l	length (m)
M	molecular weight (kg/mol)
Q	heat per unit time (J/s)
$\dot{r}$	rate of reaction (mol/m^3/s)
T	temperature (K)
u	velocity (m/s)
V	reactor volume (m^3)
x	axial coordinate (m)
Y	mass fraction

Greek symbols

ν	stoichiometric coefficient
ρ	density (kg/m^3)

Subscripts and superscripts

g	gas phase
j	reaction index
k	species index
s	solid wall
∞	external/environmental conditions
0	inlet conditions

very simple, it did extremely well in qualitatively predicting the quenching behavior. The same authors [23] also used a transient one-dimensional (1D) model to examine the role of reactor structure and gap width on quenching behavior.

The aim of this paper is to extend prior work of our group [20,21], by presenting a more comprehensive study about the effect of reactor dimensions and operating conditions on thermal quenching. An important question is whether there is an optimal gap size, reactor structure thickness and reactor length that enhance flame stability. To efficiently explore parameter space and get further insights into flame stability for fabricating micro- and meso-scale burners, a computationally more tractable 1D model is employed, instead of a CFD model. The effects of wall thermal conductivity and heat losses on the quenching mechanisms, and their implications on optimal reactor geometry are studied for both methane and propane fuels.

2. Reactor model

2.1. One-dimensional (1D) model

A schematic of the reactor modeled in this work is shown in Fig. 1. The reactor consists of two parallel plates of thickness

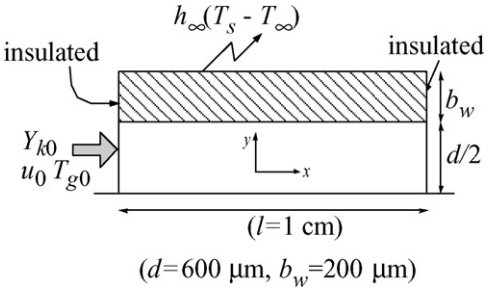

Fig. 1. Schematic of the parallel-plate reactor modeled in this work, with the plane of symmetry shown as the dash-dot line. The numbers in parentheses are the nominal values of the reactor dimensions.

b_w and length l, separated by a gap width d between them. The nominal reactor dimensions are indicated in the figure. The physical system is same as that considered in our earlier work [20,21]. This is a relatively simple geometry used in order to illustrate the primary mechanisms leading to flame quenching. It is expected that entrance effects, caused for example by different nozzles and reactor shapes, may affect microburner stability and should be studied using 2D/3D CFD simulations. The flow is laminar, and the reactants and products are assumed to be ideal gases. Owing to the large aspect ratio (l/d) of the reactor, radiation effects are neglected [24]. The steady state 1D model consists of the following continuity, mass, and energy balance equations:

$$\frac{\mathrm{d}}{\mathrm{d}x}\rho u = 0 \tag{1}$$

$$\rho u \frac{\mathrm{d}}{\mathrm{d}x} Y_k = \left[\frac{\mathrm{d}}{\mathrm{d}x}\rho D_k \frac{\mathrm{d}Y_k}{\mathrm{d}x}\right] + M_k \dot{r}_k \tag{2}$$

$$\rho u \bar{c}_\mathrm{p} \frac{\mathrm{d}}{\mathrm{d}x} T_\mathrm{g} = \left[\frac{\mathrm{d}}{\mathrm{d}x} k_\mathrm{g} \frac{\mathrm{d}T_\mathrm{g}}{\mathrm{d}x}\right] + \sum_k H_k \dot{r}_k - \frac{a_\mathrm{s}}{V} h_\mathrm{g}(T_\mathrm{g} - T_\mathrm{s}) \tag{3}$$

$$0 = k_\mathrm{s} \frac{\mathrm{d}^2}{\mathrm{d}x^2} T_\mathrm{s} + h \frac{a_\mathrm{s}}{a_\mathrm{cs} l}(T_\mathrm{g} - T_\mathrm{s}) - h_\infty \frac{a_\infty}{a_\mathrm{cs} l}(T_\mathrm{s} - T_\infty). \tag{4}$$

The physical properties, such as thermal conductivity and diffusivity of the gas phase, are assumed to be constant. Based on nitrogen (dominant species in the mixture) at 1500 K, we used $k_\mathrm{g} = 0.1$ W/m K and $D = 10^{-4}$ m^2/s. Our previous work revealed that the Nusselt number remains constant at a value of 4 (used here), throughout the reactor (except in the narrow combustion region) [21]. Obviously, incorporation of a more detailed profile of Nusselt number is entirely possible, but it is not expected to substantially change model predictions. As the focus of this work is on the effect of reactor dimensions on the thermal management, a one-step homogeneous chemistry, which neglects radical quenching, is assumed for both propane and methane combustion. The following kinetic expressions developed by Westbrook and Dryer [25] were used:

$$\mathrm{C_3H_8} + 5\mathrm{O_2} \rightarrow 3\mathrm{CO_2} + 4\mathrm{H_2O}, \quad \Delta H^0 = -2070\,\mathrm{kJ/mol},$$

$$-r_\mathrm{Pr} = 4.836 \times 10^9 \exp\left(\frac{-1.256 \times 10^8}{\mathrm{RT}}\right) C_\mathrm{Pr}^{0.1} \cdot C_{\mathrm{O_2}}^{1.65} \tag{5}$$

and

$$CH_4 + 2O_2 \rightarrow CO_2 + 2H_2O, \quad \Delta H^0 = -805\,\text{kJ/mol},$$
$$-r_{Me} = 2.119 \times 10^{11} \exp\left(\frac{-2.027 \times 10^8}{RT}\right) C_{Me}^{0.2} \cdot C_{O_2}^{1.3}, \tag{6}$$

where Pr and Me stand for propane and methane respectively; activation energy is in J/kg mol/K, the concentrations in kg mol/m^3, and the reaction rate in kgmol/m^3/s. Due in part to the simplicity of the chemistry employed and the fact that radical quenching could be overcome by suitable materials preparation (at least for some materials) [15], our focus here is on thermal quenching. This approach also enables us to directly compare to our recent CFD work [20,21].

The boundary conditions involve at the inlet specified (Dirichlet) conditions, an insulated wall in the flow direction, and no flux (Neumann) conditions at the outlet, i.e.,

$$\text{at inlet,} \quad x = 0: \quad u = u_0, \qquad Y_k = Y_{k0}, \qquad T_g = T_{g_0},$$
$$\text{and} \quad \frac{dT_s}{dx} = 0 \tag{7}$$

$$\text{At outlet,} \quad x = l: \quad \frac{dY_k}{dx} = \frac{dT_s}{dx} = \frac{dT_g}{dx} = 0 \tag{8}$$

A finite difference scheme was used to discretize the model with 200 equidistant nodes and the resulting algebraic equations were solved using Newton's method. The Jacobian was computed analytically and a banded solver was used at each Newton's iteration. Once a stable solution was obtained, natural parameter continuation with respect to solid thermal conductivity (k_s), heat loss coefficient (h_∞), or inlet velocity (u_0) was employed. The solver was under-relaxed, if required, and a gradually decreasing continuation step was taken close to turning points.

2.2. Validation and benchmarking

The first task was to perform simulations using the 1D model, and to compare the results with those from the 2D CFD simulations (for details of the CFD simulation, see [20,21]). Fig. 2 shows the temperature profiles in the solid and gas phases along with the reaction rate for a stoichiometric propane–air mixture entering the reactor at $T_{g_0} = 300$ K, with an inlet velocity $u_0 = 0.5$ m/s, at atmospheric pressure. The solid thermal conductivity was $k_s = 7.5$ W/m K, the heat loss coefficient $h_\infty = 10$ W/m^2 K, and the reactor dimensions $d = 600$ μm, $b_w = 200$ μm and $l = 1$ cm. These values represent the ''nominal'' operating conditions. The lines represent 1D model responses and the symbols denote 2D model responses, averaged over the transverse direction. The axial profiles from the two models are quantitatively similar. Simulations were performed for several different values of thermal conductivity and inlet velocity using both the 1D and 2D models. The 1D model deviates slightly from the 2D model at very low and high values of wall conductivity. Fig. 3a, which is discussed in the next section, compares the quenching curves obtained for a

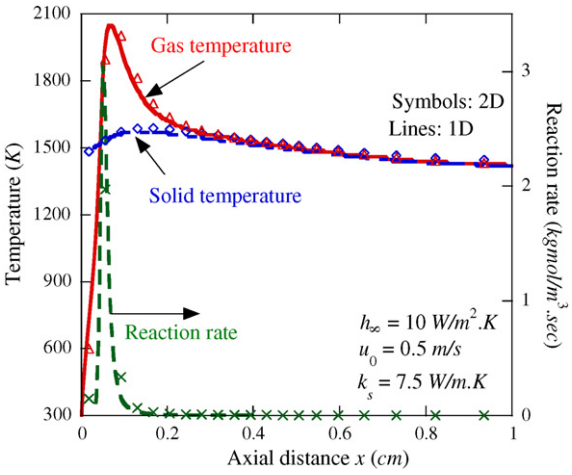

Fig. 2. Axial profiles of gas (solid line) and wall (dashed-dot line) temperatures, and reaction rate (dashed line) for stoichiometric propane–air combustion at nominal reactor dimensions of $d = 600$ μm, $b_w = 200$ μm, and $l = 1$ cm using the 1D code. The corresponding values (cup averaged) using 2D fluent simulations are shown as symbols.

stoichiometric propane–air feed at $u_0 = 0.5$ m/s. Despite substantial gradients seen in previous 2D CFD simulations [20,21] in the gas phase, heat transfer via the wall dominates operation, and as a result, the two models are in reasonable quantitative agreement to encourage further studies with the 1D model.

Use of this simplified 1D model results in significant reduction of computational time. While the CFD simulation takes 30 min to several hours for a single calculation at given conditions, parametric continuation along one parameter takes only a couple of minutes using our 1D codes. This allows us to systematically investigate parameter space for enhanced stability of self-sustained combustion in small channels.

3. Flame characteristics and quenching modes in small channels

3.1. Stability of propane–air micro-flames

The limits of stable operation of propane–air micro-combustion are depicted in Fig. 3. As mentioned in our previous work [20], a flame thermally quenches due to one of the two mechanisms: *extinction*, which refers to the case where a flame quenches because the heat released by combustion is insufficient to sustain heat losses; and *blowout*, which refers to the case where a flame gets swept out of the reactor at low residence times (i.e., high flow rates). Hereafter, in all figures, extinction will be denoted by circles, whereas blowout by squares. In previous work we distinguished between these two modes mainly based on flame location. However, additional characteristics, discussed below, serve to better elucidate the quenching mechanism.

The critical heat loss coefficient, which accounts for losses to the environment or possible heat exchange with an endothermic reaction, versus solid thermal conductivity is plotted in Fig. 3a. The figure shows a bell-shaped curve, with

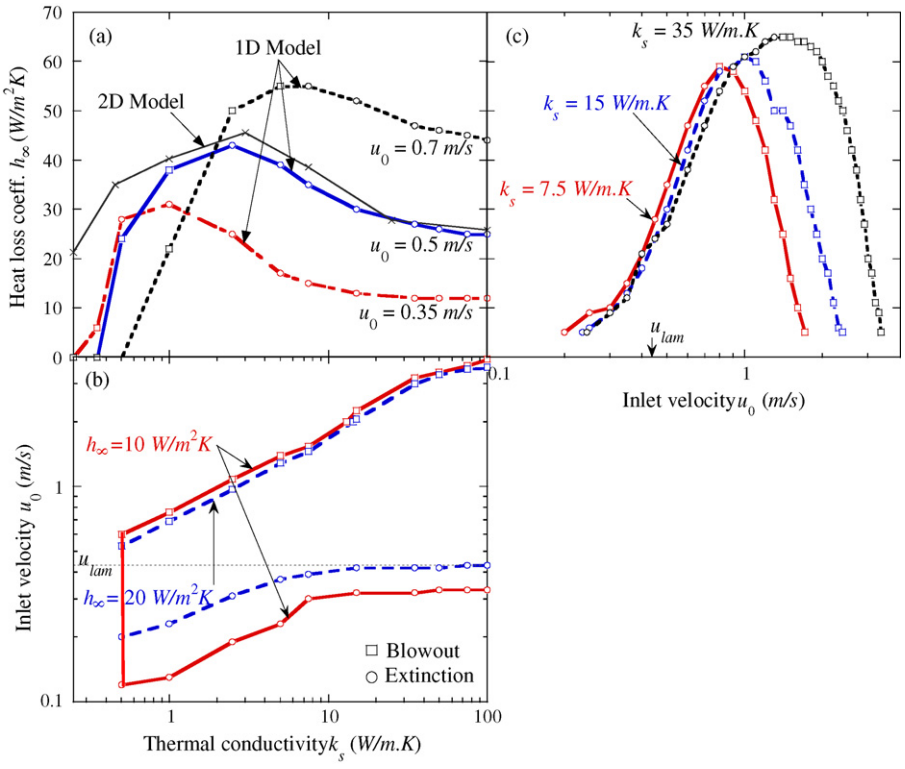

Fig. 3. Critical quenching limits for stoichiometric propane–air micro-combustion for nominal reactor dimensions of d = 600 μm, b_w = 200 μm and l = 1 cm: (a) critical heat loss coefficient vs. thermal conductivity at various inlet velocities; (b) critical inlet velocity vs. thermal conductivity curves for two values of heat loss coefficient; (c) critical heat loss coefficient vs. inlet velocity curves. Squares represent blowout, whereas circles represent extinction. The laminar burning velocity [26] is marked as u_{lam}. The corresponding k_s vs. h_∞ curve for u_0 = 0.5 m/s generated using 2D fluent simulations is shown as a thin line in panel (a) for comparison.

blowout observed at lower values of solid thermal conductivity (k_s) and extinction at higher values of k_s. The region below (above) the curve indicates self-sustained (non self-sustained) combustion. The critical values of inlet velocities are plotted as a function of k_s in Fig. 3b. The two curves delimit the region of stable combustion. The separation of extinction and blowout is clear in this figure: at each value of thermal conductivity, the former occurs at low velocities and the latter at much higher velocities. Finally, Fig. 3c depicts the critical heat loss coefficient as a function of inlet velocity. The region under the bell-shaped curve denotes stable combustion. The heat loss–velocity curves go through a maximum, which represents a transition from extinction to blowout. The velocity at which the maximum is observed as well as the maximum value of heat loss coefficient increase as the solid thermal conductivity k_s increases.

These plots underline another important point distinguishing the quenching modes. The blowout curves of Fig. 3b have a significantly larger slope than those of the extinction curves; additionally, the blowout curves for different coefficients of heat loss are close to each other. Similarly in Fig. 3c, the slopes of extinction curves are larger than those of the blowout curves, whereas the extinction curves for different k_s are close to each other. This means that the external heat loss coefficient has a strong influence on flame extinction, whereas the solid thermal conductivity has a strong effect on blowout.

Fig. 4 shows the flame characteristics as a function of inlet velocity for various values of (k_s, h_∞). The left end (circles) denotes extinction and the right end (squares) denotes blowout. Fig. 4a shows that as one approaches either of the critical limits, the flame location moves significantly downstream. Therefore, flame location may not be the best indicator of quenching mode. Yet, in blowout of propane–air flames, the flame is typically located further downstream. The conversion of propane is in excess of 90% throughout the entire range of operation (Fig. 4b); the conversion is nearly complete at blowout; but drops as one approaches extinction, due to lower temperatures, as shown in Fig. 4d. Heat loss to the surroundings shows a monotonic trend as the velocity increases from the extinction to the blowout limit. It is clear from Fig. 4c that the ratio of heat lost via the walls to the total heat generated is large at extinction, resulting in significantly lower temperatures. On the other hand, the temperature at blowout limit is much higher, approaching the adiabatic flame temperature. The heat recirculated upstream through the reactor solid structure results in stabilization of the flame. Consequently, since blowout occurs on account of the flame being swept out of the reactor at high flow rates, it depends strongly on the thermal conductivity, with more conductive materials being able to sustain higher velocities that can far exceed the laminar flame speed (u_{lam}) due to heat recirculation (see Fig. 3b).

An important point to take away from Fig. 4 is that a substantial fraction of the heat generated gets lost even at moderate values of the heat loss coefficient (in the natural convection range). Operation at faster flow rates toward the blowout limit decreases this fraction (Fig. 4c) and can be an important strategy in designing portable devices with maximum energy efficiency; however, at the cost of higher solid

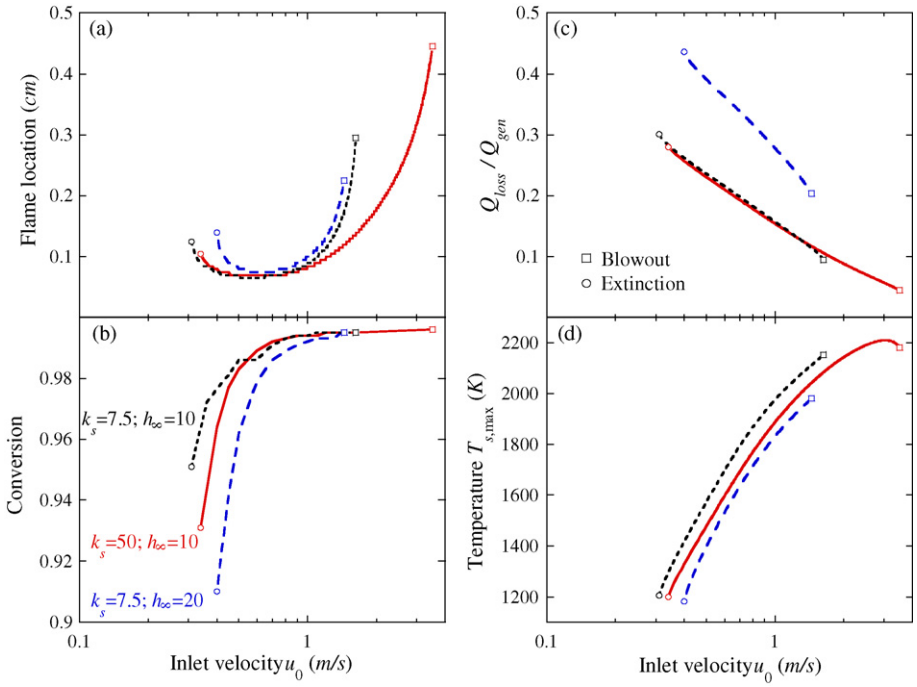

Fig. 4. Characteristic curves for stoichiometric propane–air combustion as a function of inlet velocity: (a) location of flame within the reactor, (b) propane conversion, (c) the ratio of heat lost through the solid plates to heat generated by combustion, and (d) maximum solid temperature. The circles denote the extinction and the squares the blowout limits. The units of k_s are W/m K and those of h_∞ are W/m^2 K.

wall operating temperatures (Fig. 4d) that may be difficult to handle from the materials point of view. Finally, for microreactors of highly conductive walls, stability limit at extinction is extended for faster flows (see Fig. 3a) due to the decreased fraction of heat loss stemming from the higher enthalpy per unit time flowing into the system inlet and the shorter residence time of gases that minimizes heat losses.

3.2. Effect of fuel

To study the effect of hydrocarbon fuel, simulations were performed for methane fuel and the results compared with those of propane. Fig. 5 shows the maximum wall temperature versus the inlet gas temperature for stoichiometric propane–air and methane–air mixtures. Propane has a higher energy density per unit volume and lower activation energy for homogeneous combustion than methane. As a result, the methane flame temperature is lower and its ignition temperature is higher. Therefore, the window of stable methane combustion is narrower than that for propane. Fig. 6 shows the critical limits for stable self-sustained combustion of stoichiometric methane–air mixtures, with the critical heat loss coefficient plotted against wall conductivity and inlet velocity in panels (a) and (b), respectively. The corresponding critical heat loss–wall conductivity curve for propane is shown as a thin dotted line for comparison in Fig. 6a. The overall trend for extinction of methane is similar to that seen for propane; however, extinction happens at much lower values of heat loss coefficient. Likewise, blowout occurs at much lower velocities than what was observed for propane. However, there is a qualitative difference between blowout characteristics of methane and propane, in that the blowout limit is only weakly dependent on the wall conductivity for methane in contrast to propane.

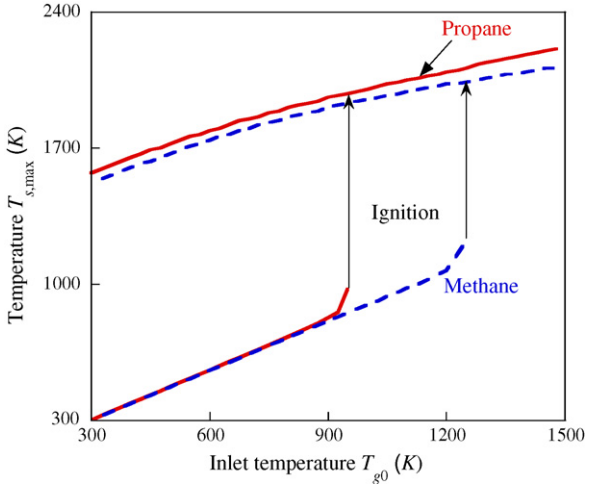

Fig. 5. Bifurcation plot showing ignition of propane and methane in a microreactor. The relevant parameters are the same as in Fig. 2. The methane ignition temperature is higher and the flame temperature lower than those of propane.

Fig. 7 shows the flame location and the fractional heat loss over the heat generation (Q_{loss}/Q_{gen}) for methane combustion spanning the velocity range of stable operation. The corresponding curve for propane is also plotted as a thin dotted line for comparison. The fractional heat loss and temperature curves (not shown) for methane and propane are similar to each other. However, the methane flame is located more downstream as compared to propane, as a larger distance from the entrance is required to reach methane's higher ignition temperature. This perhaps makes the methane flame more

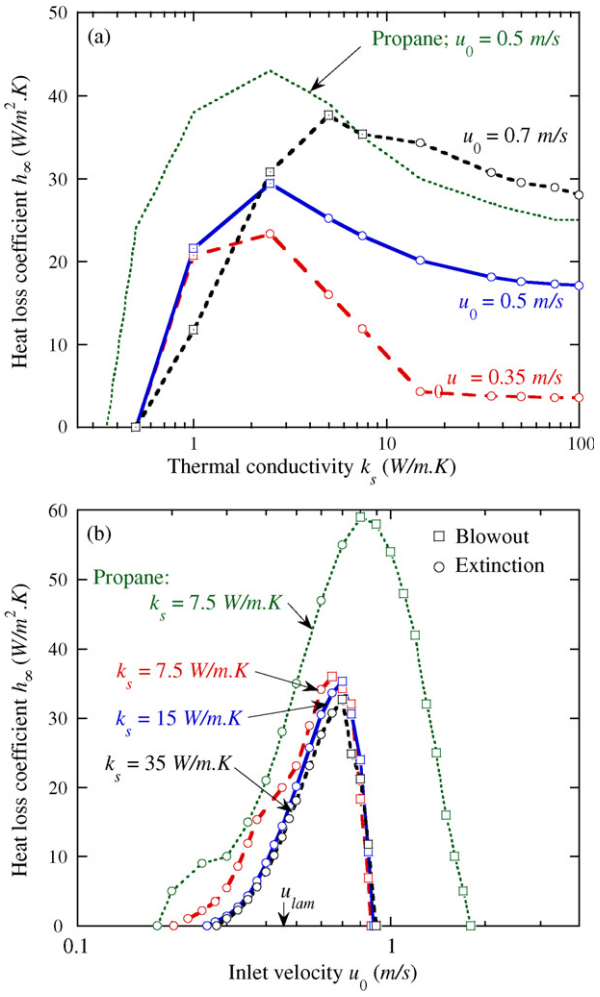

Fig. 6. Extinction characteristics for stoichiometric methane–air mixtures. The parameters are as in Fig. 3. The critical heat loss curves for propane at u_0 = 0.5 m/s and k_s = 7.5 W/m K are plotted as thin dotted lines for comparison. The maximum heat loss coefficient and the maximum velocity for stable operation of methane combustion are lower than those of propane.

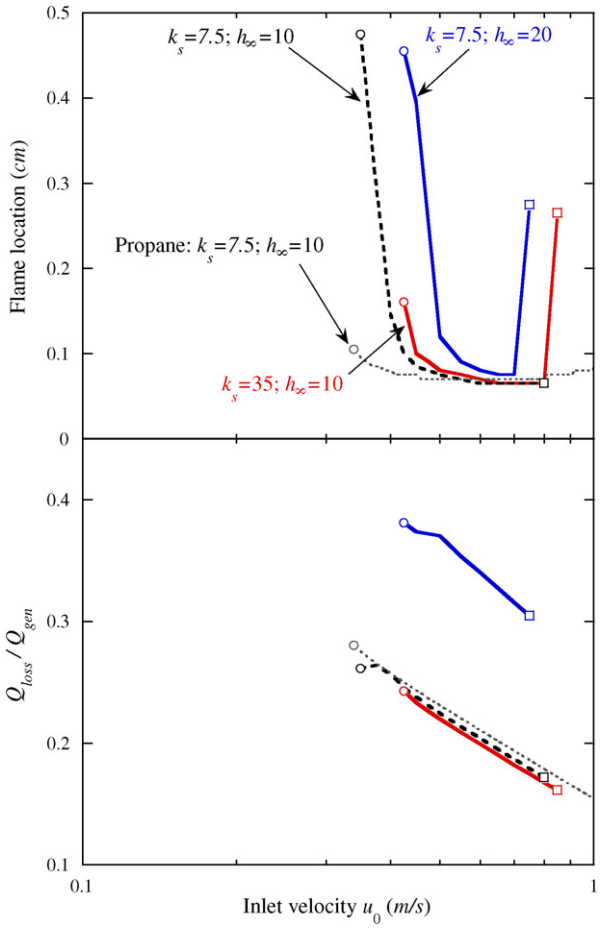

Fig. 7. Flame location and fractional heat loss plotted as a function of inlet velocity for a stoichiometric methane–air system. Circles represent extinction and squares represent blowout. The corresponding curve for propane is shown as a thin dotted line for comparison, with the abscissa truncated to highlight methane data. Units of k_s are W/m K and h_∞ are W/m^2 K.

prone to blowout (see Figs. 7 and 6b), and a faster heat recirculation through more conducting walls is unable to increase the blowout limit, as was observed in propane.

Norton and Vlachos [21] performed a kind of sensitivity analysis by substituting the reaction rate and energy density of propane with those of methane (they called this a pseudo-fuel). Their conclusion that the difference in the quenching characteristics of the two fuels is mainly due to the difference in their activation energies is consistent with the results presented in this section. Based on this, we postulate that fuels or fuel blends that have a lower ignition temperature will result in a more stable reactor operation.

4. Effect of reactor geometry

It is expected that in small-scale systems, surface phenomena dominate over bulk phenomena. In the previous section, we saw that the reactor solid structure has a profound effect on the thermal stability of micro-combustion, as it is the main route for heat dissipation with multiple effects: namely, reducing the peak solid temperatures, controlling heat loss, and recirculating the heat upstream that is critical for ignition. There is an interplay between higher heat losses versus higher heat recirculation or higher residence times as the wall thermal conductivity and reactor size change. It is not immediately clear what are the appropriate scales of reactor gap width, reactor length, and thickness of reactor walls, and these effects are investigated next for propane–air first and methane–air last.

4.1. Reactor gap width

The rate of convective heat transfer to the reactor walls is linearly dependent on the inverse of the gap width. Increased heat transfer to the walls by shrinking the gap width results in an increase in heat recirculation as well as an increase in heat losses. Fig. 8 shows the critical heat loss coefficient as a function of solid thermal conductivity (panel a) and inlet velocity (panel b) for different gap widths. An important observation in Fig. 8a is that the dominant quenching

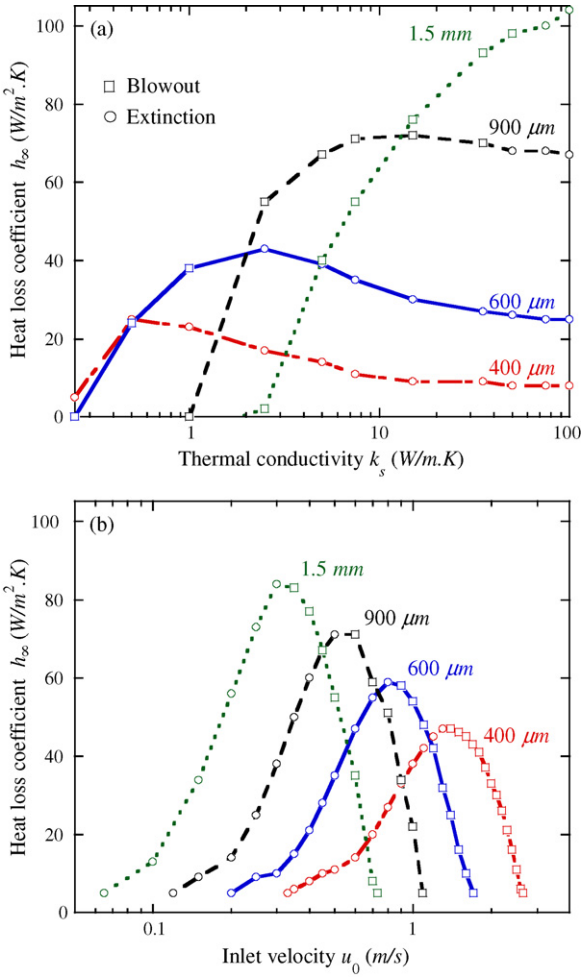

Fig. 8. Effect of reactor gap width on quenching characteristics for stoichiometric propane–air combustion. Critical values of heat loss coefficient are plotted against: (a) solid thermal conductivity for $u_0 = 0.5$ m/s; (b) inlet velocity for $k_s = 7.5$ W/m K. Larger channels can sustain combustion at higher heat losses for highly conductive materials, whereas smaller channels are more stable for very insulating materials.

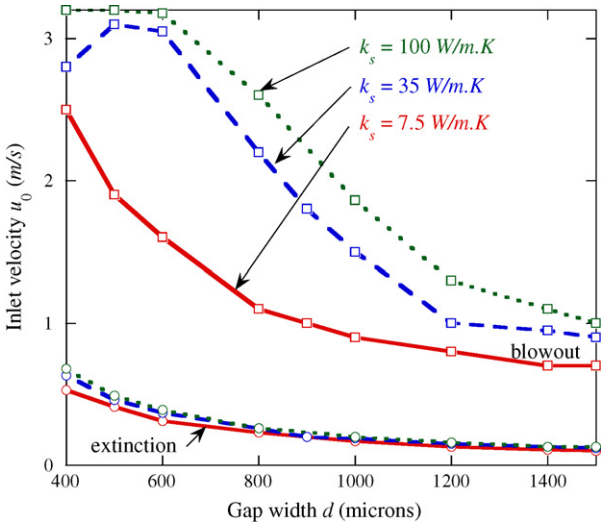

Fig. 9. Critical values of inlet velocity are plotted as a function of gap width for solid thermal conductivities of $k_s = 7.5$ W/m K (solid line), $k_s = 35$ W/m K (dashed line), and $k_s = 100$ W/m K (dotted line), and heat loss coefficient value of $h_\infty = 10$ W/m^2 K for stoichiometric propane–air combustion.

mechanism changes with varying gap size: small channels quench because of extinction (heat loss) due to large surface to volume ratio and fast heat transfer, whereas larger channels suffer mainly from blowout due to insufficient heat recirculation (note that the circles denote extinction whereas squares blowout). This change in quenching mechanisms has important ramifications on the effect of gap size on stability. Based on intuitive thermal quenching arguments, one may expect combustion to be more stable for larger gap widths. However, Fig. 8a reveals that for reactors having walls with low thermal conductivity (such as ceramics), reactors with sub-millimeter gap width may actually be more stable than those with larger gap width (e.g., compare 400 μm to 1.5 mm for $k_s = 7.5$ W/m K). This behavior is in contrast to highly conducting walls, wherein high heat recirculation allows relatively higher velocities to be sustained (without blowout occurring) in reactors with larger gap widths. At very small gap widths (e.g., 400 μm or lower), extinction occurs at relatively low values of heat loss coefficient. As the gap width increases, flames become more stable to heat losses. As the gap width is increased beyond 1 mm (meso-scale), blowout becomes prominent for poorly conducting walls and results in reduced stability of self-sustained combustion. There seems to be an "optimum size," which occurs at the transition from micro- to meso-scales (i.e., at ∼1 mm). Fig. 8b shows that the heat loss–inlet velocity curves qualitatively maintain their shape, but just move towards lower velocity values as the gap width is increased. In other words, the maximum power generated could be controlled by tuning the gap width.

Fig. 9 presents an alternate view of the quenching characteristics described above, by plotting the critical velocities as a function of gap width. It is to be noted that the velocity scale (ordinate) is linear, and not logarithmic as in Fig. 8b. It is evident that the extinction limit is relatively insensitive to the gap size, whereas the blowout limit varies significantly with gap size. For low conductivity ceramics, the blowout limit decreases monotonically with increasing gap size over the scales explored. For intermediate conductivity materials, a maximum occurs at ∼600 μm, and for highly conductive materials, a plateau is seen below a certain size when apparently the time scales for heat transfer from the gas to the wall and within the wall are sufficiently short. The operating window becomes narrower due to a decrease in the critical velocity for blowout, as the meso-scale regime is approached, and thus, small gap sizes are better for higher flow velocities (and powers). Fig. 10 plots the critical value of heat loss coefficient as a function of gap width. This plot clearly shows that there exists an optimal gap width regarding flame stability for low to moderate conductivities, for which the critical value of h_∞ exhibits a maximum. As the thermal conductivity k_s increases, the optimal gap width also increases. In summary, gap widths in the range 600–1200 μm are ideal for enhanced stability depending on material and flow velocity.

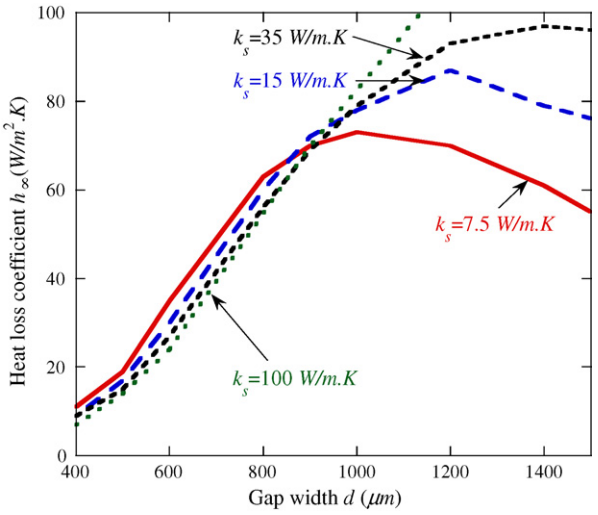

Fig. 10. Maximum value of the heat loss coefficient as a function of gap width for an inlet velocity of $u_0 = 0.5$ m/s and different values of solid thermal conductivity, as in Fig. 9, for stoichiometric propane–air combustion.

Fig. 11 shows the flame location and fractional heat loss as a function of inlet velocity, for different reactor dimensions. The two dashed lines indicate reactors with the same length and different gap widths as the nominal reactor (solid line). For the same operating conditions, the reactor with the larger gap width experiences a smaller relative heat loss, and is consequently more stable against extinction. In contrast, the flame is located significantly downstream, and therefore, blowout occurs at a much lower value of inlet velocity.

Methane also shows similar quenching behavior with respect to the gap width (Fig. 12). Consistent with one's expectations, gap width has a more profound effect on flame stability for self-sustained methane combustion. A major difference in methane–air combustion is that the extinction is a strong function of gap width at small gap widths, causing the operating window to shrink significantly as the gap width decreases below 500 μm. In these narrower channels, a larger portion of heat gets transferred from the gas to the solid, a part of which is lost to the surroundings. An increased heat loss causes methane flames to move significantly downstream, before finally approaching the extinction limit (also see Fig. 7). Hence, for homogeneous methane combustion, reactors should not be designed with gap widths less than 500 μm. Similar to propane, a gap width of approximately 1 mm provides the largest operating window.

4.2. Plate/structure thickness

The reactor solid structure affects both the rate of heat transfer upstream and the rate of heat loss. Owing to the small plate thickness, resistance to heat transfer in the transverse direction due to the solid reactor structure is negligible as compared to the effect of external heat loss coefficient, h_∞. As a result, the plate thickness b_w primarily affects the axial heat transfer upstream in the reactor. The thicker the plate, the larger is the area available for axial heat transfer. Thus, doubling the

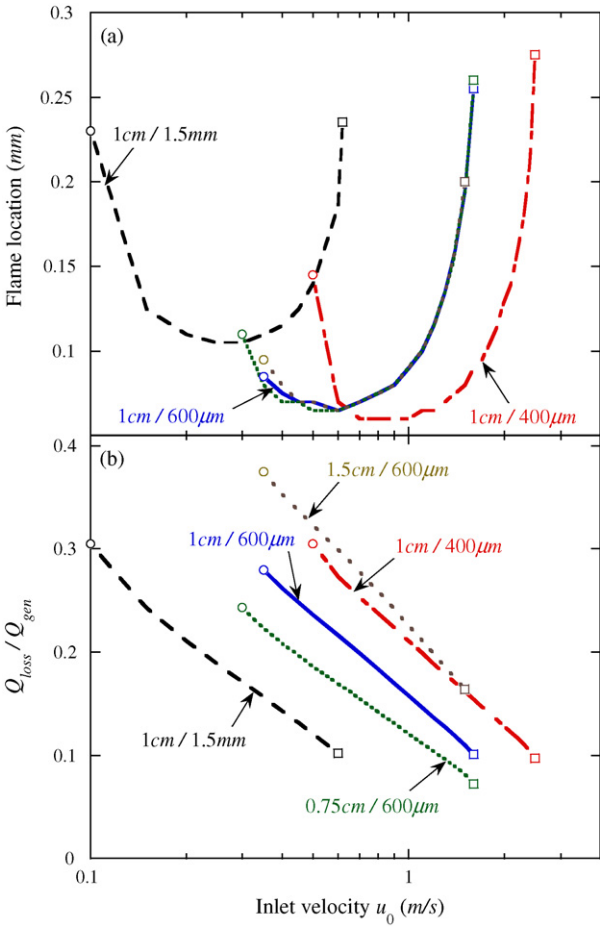

Fig. 11. Flame location (panel a) and fractional heat loss (panel b) are plotted as a function of inlet velocity for $k_s = 7.5$ W/m K and $h_\infty = 10$ W/m^2 K, and for various gap widths and reactor lengths for stoichiometric propane–air combustion. The solid line represents the nominal reactor dimensions (l/d) = (1 cm/600 μm). The two dotted lines represent reactors with the same gap width but different lengths (0.75 and 1.5 cm); the two dashed lines indicate reactors with the same length but different gap widths (400 and 1500 μm).

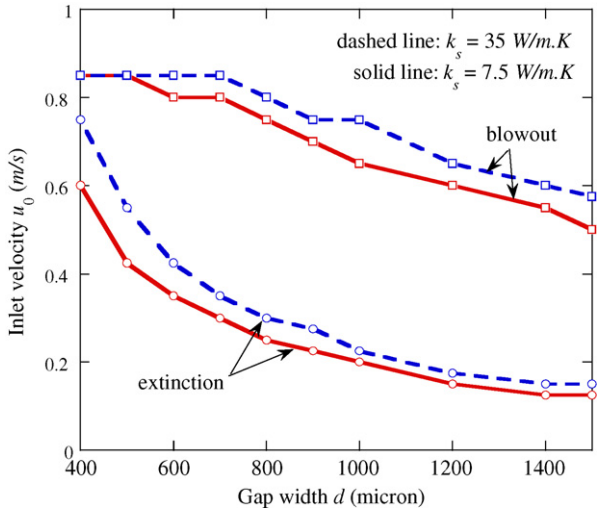

Fig. 12. Effect of gap width for stoichiometric methane–air combustion. A gap width of about 1 mm provides the largest operating window for homogeneous methane combustion in small channels.

plate thickness has quantitatively the same effect as that of doubling the thermal conductivity.

Investigation of Eq. (4) indicates that the specific surface area in the last two terms is $1/b_w$. Multiplying by b_w, it is clear that the product $k_s b_w$ is important. For a general case of a reactor with an arbitrary geometry, the product $k_s a_{cs}$, where a_{cs} is the cross-sectional area of the solid body, is critical. This product is sometimes called thermal conductance.[1] For the sake of brevity, no additional figures are provided. However, the same plots (Figs 3 and 6) can be used by changing the abscissa from thermal conductivity to thermal conductance, with the value of $b_w = 200$ μm.

4.3. Reactor length

A longer reactor provides a larger residence time that could allow for more complete, and thus, more stable combustion, especially towards the blowout limit. However, the effect of reactor length on propane combustion in Fig. 13 shows that the situation is not so straightforward. A longer reactor provides a larger surface area for heat loss. Hence, other operating conditions remaining the same, the fractional heat loss is higher for a longer reactor than a shorter one. Consequently, extinction takes place at lower values of external heat loss coefficient in a longer reactor and the region of stable operation shrinks. Increasing the reactor length does not significantly increase the blowout limit for most of the range of wall conductivities of practical interest (such an increase occurs for $k_s \ll 1$ W/m K, as shown in Fig. 13a).

The reason for these effects becomes clearer from Fig. 11. The two dotted lines represent reactors with the same gap width but different lengths than the nominal (solid line) case (these lines are difficult to discern in Fig. 11a). The amount of heat loss increases significantly with an increase in the reactor length, thus resulting in shrinking of the extinction limit. Fig. 11a shows the flame location for three different lengths. The actual location of the flame is almost independent of the reactor length. The flame is located within the initial 0.1 cm of the reactor for most of the range of velocities. Close to the blowout limit, the flame location increases steeply before getting blown out. Thus, only a small increase, if any, in the maximum velocity is observed when the reactor length is increased. Therefore, a longer reactor does not result in any significant stabilization of the blowout limit. An exception to this behavior is observed for highly insulating walls (e.g., $k_s = 0.5$ W/m K), wherein the low thermal conductivity limits the upstream heat transfer. A longer reactor can enhance the flame stability by providing a larger residence time.

Similar results were obtained for methane, but are skipped for brevity. Since methane flames get quenched in reactors with highly insulating walls, an analogous improvement of flame stability with an increase in length was not observed.

[1] Thermal conductance is not a standard term. Sometimes, the inverse of thermal resistance, i.e. $k_s a_{cs}/l$, is called thermal conductance instead of the definition used here.

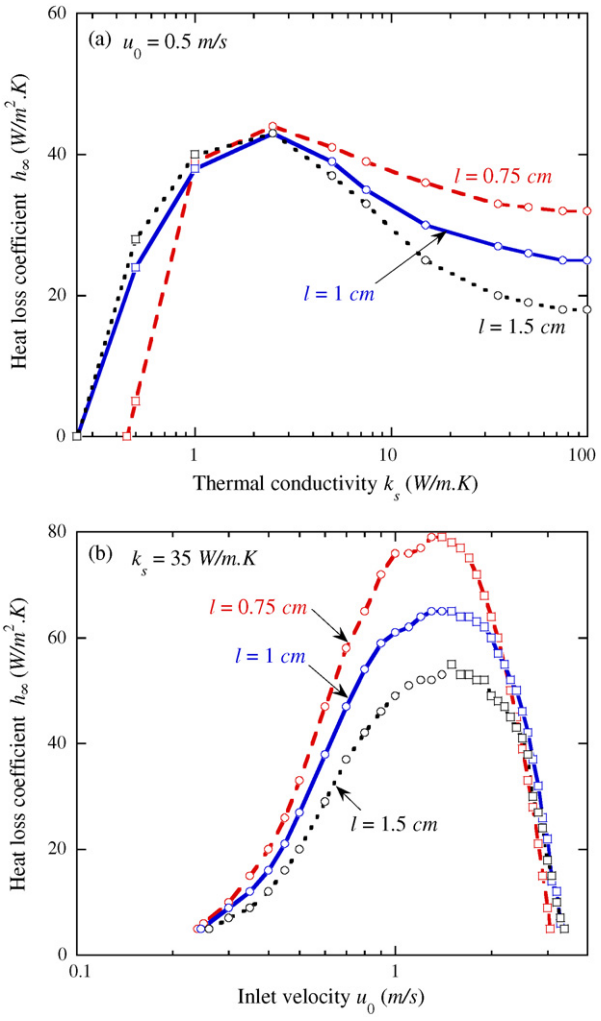

Fig. 13. Effect of reactor length on flame stability. Combustion is stable for higher heat loss coefficients in shorter reactors with moderate to high conductivity walls. This is because for the same heat loss coefficient, longer reactors result in higher total heat loss. Conversely, a slightly increased stability is observed for the blowout limit for longer reactors with low conductivity wall materials.

5. Conclusions

In this paper, we build on the insights obtained in our previous work [20,21] on the flame characteristics and stability of propane and methane combustion in small-scale channels. Specifically, the effect of reactor dimensions and system parameters on the two mechanisms of thermal quenching of premixed flames, viz. extinction and blowout, were studied using an efficient 1D model. While a parallel plate geometry was investigated, qualitatively similar results should hold for other geometries. The following insights were obtained regarding the mechanisms of extinction and blowout, and the effect of thermal conductivity and heat losses on them:

- Extinction occurs when the heat released by reaction is insufficient to sustain combustion due to heat loss. As a result, at the extinction limit, the ratio of heat losses to the total heat generated is high and the maximum temperature is low.

Blowout, on the other hand, occurs because the flame gets swept out of the reactor at higher velocities due to lower residence times. The heat losses are comparatively lower and the maximum temperatures higher at the blowout limit.

- Heat recirculation through the reactor solid structure is mainly responsible for stabilizing flames in small channels. Therefore, the solid thermal conductivity has a stronger effect on the blowout limit and a relatively weaker effect on the extinction limit. Higher thermal conductivity materials make it possible to operate a microreactor at higher inlet velocities (and therefore higher powers), even above the flame speed; however, extinction occurs at lower values of the heat loss coefficient.
- Extinction is strongly affected by heat losses to the surroundings, while blowout shows relatively weaker dependence on heat losses. Maximum heat losses are sustainable in reactors made with materials having thermal conductivity of 1–10 W/m K, depending on flow velocity.

The second contribution of this paper is to understand the effect of reactor dimensions on flame stability. The effect of reactor length, gap size, and plate thickness are summarized below:

- Increasing the reactor length results in an increase in heat loss (for the same value of external heat transfer coefficient) and residence time. Thus, longer reactors tend to get extinguished at lower critical values of the heat loss coefficient. As a result, shorter reactors are preferable while operating closer to the extinction limit. An exception is propane–air (though not methane–air) combustion in reactors with highly insulating walls (typically a non-practical situation), where longer reactors are more stable.
- Thicker reactor walls provide a larger area for axial heat conduction and have the same effect as that of increasing the thermal conductivity. As a result, higher velocities can be sustained in reactors of lower thermal conductivity solids using thicker walls.
- The channel gap width has a strong effect on quenching limits that is fuel dependent. The rate of heat transfer to the wall has an approximately linear dependence on the inverse of gap width. Thus, when the gap width is reduced, the net heat loss as well as the heat recirculation towards the upstream of the reactor increase. The former makes the flames less stable near the extinction limit, whereas the latter stabilizes the flames at higher velocities allowing blowout to occur at much higher velocities. There appears to be an optimum gap width in the micro- to meso-scale range (600–1200 μm) for enhanced flame stability. However, materials integrity in terms of high wall temperatures should also be carefully considered in design.
- The effect of these parameters is even more profound for methane than for propane. This is generally attributed to the higher ignition temperature of methane.

The model employed herein is a steady state one; transients are obviously important since many microscale devices operate in an on/off mode. Furthermore, periodic operation could enhance flame stability. These issues will be addressed in forthcoming communications.

Acknowledgements

This work was supported by the Army Research Office under Contract DAAD19-01-1-0582. Any opinions, findings, and conclusions or recommendations expressed are those of the authors and do not necessarily reflect the views of the Army Research Office.

References

[1] A.C. Fernandez-Pello, Micropower generation using combustion: issues and approaches, Proc. Combust. Inst. 29 (2003) 883–889.
[2] N. Edwards, S.R. Ellis, J.C. Frost, S.E. Golunski, A.N.J. van Keulen, N.G. Lindewald, J.G. Reinkingh, On-board hydrogen generation for transport applications: the hotspot (tm) methanol processor, J. Power Sources 71 (1998) 123–128.
[3] J.D. Holladay, E.O. Jones, M. Phelps, J.L. Hu, Microfuel processor for use in a miniature power supply, J. Power Sources 108 (2002) 21–27.
[4] A.V. Pattekar, M.V. Kothare, A microreactor for hydrogen production in micro fuel cell applications, J. Microelectromech. Syst. 13 (2004) 7–18.
[5] J.C. Ganley, E.G. Seebauer, R.I. Masel, Porous anodic alumina microreactors for production of hydrogen from ammonia, AIChE J. 50 (2004) 829–834.
[6] S.R. Deshmukh, D.G. Vlachos, Effect of flow configuration on the operation of coupled combustor/reformer microdevices for hydrogen production, Chem. Eng. Sci. 60 (2005) 5718–5728.
[7] I.A. Waitz, G. Gauba, Y. Tzeng, Combustors for micro gas turbine engines, J. Fluids Eng. 120 (1998) 109–117.
[8] J. Peirs, D. Reynaerts, F. Verplaetsen, A microturbine for electric power generation, Sens. Actuators A 113 (2004) 86–93.
[9] S.B. Schaevitz, A.J. Franz, K.F. Jensen, M.A. Schmidt, in: Proceedings of the 11th International Conference on Solid-State Sensors and Actuators, Munich, Germany, 2001.
[10] J.A. Federici, D.G. Norton, T. Bruggemann, K.W. Voit, E.D. Wetzel, D.G. Vlachos, Catalytic microcombustors with integrated thermoelectric elements for portable power production, J. Power Sources, 2006, in press, doi:10.1016/j.jpowsour.2006.06.042
[11] W.M. Yang, S.K. Chou, C. Shu, Z.W. Li, H. Xue, A prototype microthermophotovoltaic power generator, Appl. Phys. Lett. 84 (2004) 3864–3866.
[12] H. Davy, Some researches on flame, Phil. Trans. Roy. Soc. Lond. 107 (1817) 45–76.
[13] A. Linan, F.A. Williams, Fundamental Aspects of Combustion, Oxford University Press, New York, 1993.
[14] P. Aghalayam, P.-A. Bui, D.G. Vlachos, The role of radical wall quenching in flame stability and wall heat flux: hydrogen-air mixtures, Combust. Theory Model. 2 (1998) 515–530.
[15] C.M. Miesse, R.I. Masel, C.D. Jensen, M.A. Shannon, M. Short, Submillimeter-scale combustion, AIChE J. 50 (2004) 3206–3214.
[16] K. Maruta, K. Takeda, J. Ahn, K. Borer, L. Sitzki, P.D. Ronney, O. Deutschmann, Extinction limits of catalytic combustion in microchannels, Proc. Comb. Inst. 29 (2003) 957–963.
[17] P.D. Ronney, Analysis of non-adiabatic heat-recirculating combustors, Combust. Flame 135 (2003) 421–439.
[18] Y. Ju, C.W. Choi, An analysis of sub-limit flame dynamics using opposite propagating flames in mesoscale channels, Combust. Flame 133 (2003) 483–493.
[19] S. Raimondeau, D.G. Norton, D.G. Vlachos, R.I. Masel, Modeling of high temperature microburners, Proc. Combust. Inst. 29 (2003) 901–907.
[20] D.G. Norton, D.G. Vlachos, Combustion characteristics and flame stability at the microscale: a cfd study of premixed methane/air mixtures, Chem. Eng. Sci. 58 (2003) 4871–4882.

[21] D.G. Norton, D.G. Vlachos, A CFD study for propane/air microflame stability, Combust. Flame 138 (2004) 97–107.
[22] T.T. Leach, C.P. Cadou CP, G.S. Jackson, Effect of structural conduction and heat loss on combustion in micro-channels, Combust. Theory and Modelling 10 (2006) 85–103.
[23] T.T. Leach, C.P. Cadou, The role of structural heat exchange and heat loss in the design of efficient silicon micro-combustors, Proc. Comb. Inst. 30 (2005) 2437–2444.
[24] N.S. Kaisare, J.H. Lee, A.G. Fedorov, Hydrogen generation in a reverse-flow microreactor. 1. Model formulation and scaling, AIChE J. 51 (2005) 2254–2264.
[25] C.K. Westbrook, F.L. Dryer, Simplified reaction mechanisms for the oxidation of hydrocarbon fuels in flames, Combust. Sci. Technol. 27 (1981) 31–43.
[26] K.K. Kuo, Principles of Combustion, John Wiley & Sons, New York, 1986 .